



## Energy flow and management of a hybrid wind/PV/fuel cell generation system

Thanaa F. El-Shatter \*, Mona N. Eskander, Mohsen T. El-Hagry

*Electronics Research Institute, National Research Center, Tahrir Street, Dokki, Giza 12622, Egypt*

Received 6 July 2004; received in revised form 4 January 2005; accepted 29 June 2005

Available online 29 November 2005

---

### Abstract

In this paper, an energy system comprising three energy sources, namely PV, wind and fuel cells, is proposed. Each of the three energy sources is controlled so as to deliver energy at optimum efficiency. Fuzzy logic control is employed to achieve maximum power tracking for both PV and wind energies and to deliver this maximum power to a fixed dc voltage bus. The fixed voltage bus supplies the load, while the excess power feeds the water electrolyzer used to generate hydrogen for supplying the fuel cells. A management system is designed to manage the power flow between the system components in order to satisfy the load requirements throughout the whole day. A case study is done using practical data from the El-Hammam site (40 km west of Alexandria, Egypt). The study defines the power generated by the wind and PV systems, the generated hydrogen used and stored in tanks and the power generated by the fuel cells to supply the deficiency in the load demand. Simulation results, done for two seasons, proved the accuracy of the fuzzy logic controllers. Also, a complete description of the management system is presented.

© 2005 Elsevier Ltd. All rights reserved.

*Keywords:* Fuel cell; Solar cell; Power management; Modeling; Wind; Hybrid system

---

\* Corresponding author. Tel.: +20 2 3310512; fax: +20 2 3351631.

E-mail address: [thanaa@eri.sci.eg](mailto:thanaa@eri.sci.eg) (T.F. El-Shatter).

## 1. Introduction

Global environmental concerns and the ever increasing need for energy, coupled with steady progress in renewable energy technologies, are opening up new opportunities for utilization of renewable energy resources. In particular, advances in wind and PV energy technologies have increased their use in hybrid wind/PV configurations. Integrating PV and wind energy sources with fuel cells, as a storage device replacing the conventional lead-acid batteries, leads to a non-polluting reliable energy source. The fuel cell generation system offers many advantages over other generation systems: low pollution, high efficiency, diversity of fuels, reusability of exhaust heat and on site installation.

In this paper, a 4.5 kW peak, stand alone hybrid wind–PV–fuel cell energy system for supplying a 72 V dc voltage load is designed. The system incorporates a water electrolyzer and storage tank to supply the fuel cell stack with hydrogen. The dc power required for hydrogen generation is supplied through the dc bus during surplus PV/wind power. The generated hydrogen is stored in tanks to be utilized by the fuel cells when the PV and wind energy sources fail to supply the load demand.

The wind energy conversion system (WECS) incorporated in the proposed scheme consists of a wind turbine coupled to a permanent magnet synchronous generator. An ac–dc power electronic interface with diode bridge rectifier and two dc–dc buck boost converters are used for maximum power tracking (MPT) and dc output voltage regulation. Two fuzzy logic controllers (FLC) are designed to adjust the duty cycles of the two buck boost converters to achieve MPT and output voltage regulation. This scheme differs from previous schemes [1,2] in that simultaneous MPT and voltage regulation are attained, and a different control algorithm is proposed.

The photovoltaic (PV) array interconnected with the proposed scheme consists of 40 polycrystalline silicon solar cells modules, each of them delivering 56 W peak power. Two dc–dc buck boost converters are used to deliver the maximum power point (MPP) and dc output voltage regulation. The MPPs are determined on line using the fuzzy regression model [3–6]. The MPP and output voltage regulation are achieved through the application of the fuzzy logic controller (FLC).

Managing the flow of energy throughout the proposed system to assure continuous supply of the load demand is done. The main objective of the power management system is to supply the load with its full demand while monitoring the pressure in the hydrogen tank (hydrogen threshold pressure “PTH”). Such aim is achieved through the following steps:

1. Monitoring the state of the stored hydrogen, as well as that of the wind and solar power generated and comparing them with the load demand.
2. Issue commands to the fuel cells control valves and the control circuits to control the power flow to the load.
3. Issue commands to operate the electrolyzer in order to use the excess energy to generate hydrogen for future use, i.e. when needed.

## 2. System description

The proposed system is composed of the following subsystems:

1. A 2.25 kW wind energy conversion system with fuzzy logic controllers.

2. A 2.24 kW PV array subsystem.
3. An electrolyzer for hydrogen generation when the generated power exceeds the load demand.
4. Hydrogen storage tank.
5. Fuel cells stack to supply load when wind/PV system generated power is insufficient.
6. Load.
7. Managing system incorporating valves and switches controlled digitally to achieve continuous supply of load demand.

### 2.1. Wind energy conversion subsystem (WECS)

The block diagram of the wind energy system adopted in this paper is shown in Fig. 1. It consists of a horizontal axis wind turbine coupled to a permanent magnet synchronous generator. An ac–dc power electronic interface with diode bridge rectifier and two dc–dc buck boost converters are used to track and extract maximum power available from the wind energy system (WES) for a given wind velocity and deliver this power to a 72 V dc constant voltage load. The system is designed to achieve maximum power tracking (MPT) and output voltage regulation within a wide range of wind speed variation (3–8 m/s) by means of two fuzzy logic controllers (FLC). The first FLC is designed to vary the on time “ $d_1$ ” of the switching device of the first buck boost converter (BB1) as the wind speed changes in order to achieve MPT within the considered wind speeds range. The second FLC is designed to output the on time “ $d_2$ ” of the switching device of the second buck boost converter (BB2) to achieve output voltage regulation within the same wind speed range. The subsystems modeling is described as follows:

### 2.2. Wind turbine (WT)

The power captured by the wind turbine is calculated as

$$P_w = 0.5 * C_p * \rho * \pi R^2 * V_w^3 \quad (1)$$

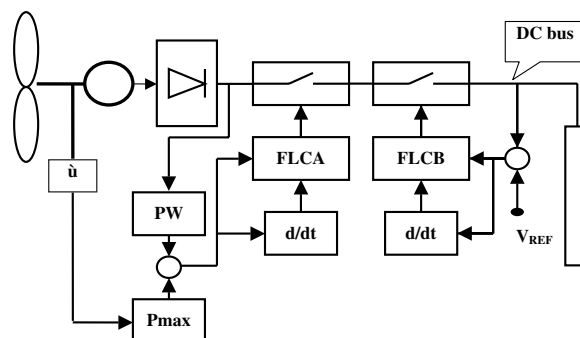


Fig. 1. Schematic of WECS with FLC.

where  $V_w$  is the average wind velocity (m/s),  $\rho$  is the air density ( $\text{kg/m}^3$ ),  $R$  is the radius of the turbine blades (m) and  $C_p$  is the power coefficient, which is a function of the tip speed ratio  $\lambda$  given by

$$\lambda = \omega_m R / V_w \quad (2)$$

where  $\omega_m$  is the rotor mechanical speed (rad/s).

To make optimal use of the available wind power, it is necessary to change the rotor speed  $\omega_m$  in proportion to the wind speed  $V_w$  to hold the value of maximum  $C_p$  as the wind speed varies. The maximum power output from the WES at different rotational turbine speeds  $\omega_m$  is computed for the considered wind turbine [7], and the data obtained is used to relate the maximum output power  $P_{\max}$  to  $\omega_m$  using a polynomial curve fit as shown below

$$P_{\max} = 0.0005 * \omega_m^3 - 0.00125 * \omega_m^2 + 0.7 * \omega_m - 74.6 \text{ W} \quad (3)$$

### 2.3. Permanent magnet synchronous generator (PMG)

A 2.25 kW, 24 pole, 500 rpm rated speed, permanent magnet generator (PMG) is employed in the WECS. The generator output voltage varies according to the wind speed variation. Hence, the 3 phase output of the PMG is rectified with a full wave diode bridge rectifier, filtered to remove significant ripple voltage components, and fed to two consecutive dc–dc buck boost converters. For an ideal PMG, the line to line voltage is given as [8]:

$$V_L = K_v \omega_e \sin \omega_e t \text{ [V]} \quad (4)$$

where  $K_v$  is the voltage constant and  $\omega_e$  is the electrical frequency related to the mechanical speed  $\omega_m$  by

$$\omega_e = \omega_m * (n_p / 2) \text{ [rad/s]} \quad (5)$$

where  $n_p$  is the number of poles of the PMG.

Neglecting commutation delays, the dc rectifier voltage  $V_d$  is given as

$$V_d = (3\sqrt{2}/\pi) * V_{L_{\text{rms}}} - (3\omega_e L_s / \pi) I_d \text{ [V]} \quad (6)$$

where  $V_{L_{\text{rms}}}$  is the rms value of the PMG output voltage,  $I_d$  is the rectifier output current and  $L_s$  is the stator inductance. Neglecting the generator and rectifier losses, the PMG output rectified electrical power  $P_{\text{dc}}$ , is equal to the mechanical power input to it

$$P_{\text{dc}} = V_d I_d \quad (7)$$

### 2.4. Buck boost converters

The two non-linear state space averaged equations describing the buck boost converters shown in Fig. 2 are [6]

$$\rho X_1 = (1 - d)/L(X_2) + d/L.U \quad (8)$$

$$\rho X_2 = -(1 - d)/C(X_1) - X_2/RC \quad (9)$$

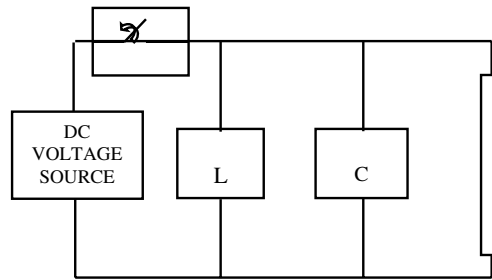


Fig. 2. Buck boost converter circuit.

where “ $d$ ” is the on time of the switching device, “ $U$ ” is the input voltage, “ $X_1$ ” is the inductor current and “ $X_2$ ” is the output voltage.

### 2.5. Fuzzy logic controllers for WECS

Because of the non-linearity of the buck boost converters, fuzzy logic controllers are applied for the MPT and output voltage regulation, providing two advantages, namely simple and robust non-linear control systems possessing features that cannot be obtained with linear controllers and, by linguistic description for the global behavior of the controllers, the need for a detailed model of the controlled system is avoided.

Two FLC are designed to achieve the following goals for the WECS:

1. Fuzzy logic controller (FLC1) varying the on time ( $d_1$ ) of the switching device of the first buck boost converter (BB1) for maximum wind power tracking. The inputs to FLC1 are chosen to be the error between the rectified actual generator power  $P_w$  and the maximum available wind power  $P_{max}$ , which is defined as “err”, and the change in this error “cerr”. FLC1 output is the value of  $d_1$ .
2. Fuzzy logic controller (FLC2) varying the on time ( $d_2$ ) of the switching device of the second buck boost converter (BB2) for regulating the output voltage of the WECS. The inputs to FLC2 are chosen to be the error between the reference voltage and the actual output voltage (err) and the change in this error (cerr). FLC2 output is the value of  $d_2$ .

Seven uniformly distributed triangular membership functions are used for the “err” input, while five uniformly distributed triangular membership functions are used for both the “cerr” and outputs for the two FL controllers. The rule base is designed such that when the error and change in error are zero, the fuzzy controller has reached the target (maximum power or regulated voltage) and is holding at it. If any disturbance occurs, the rules change to follow the maximum power and voltage reference, according to which the converter is controlled.

Fig. 3 shows the measured wind profile within 24 h in summer in the El-Hammam site, together with the output power obtained using FLC1, while Fig. 4 shows the measured wind profile within 24 h in winter in the El-Hammam site, together with the output power obtained using FLC1. It is clear in both cases that the curves of maximum available wind power coincide with the generator

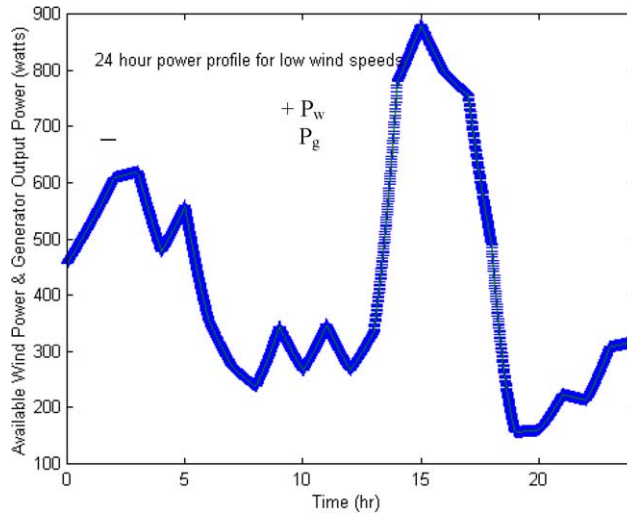


Fig. 3. Maximum power tracking for lower wind speed profile.

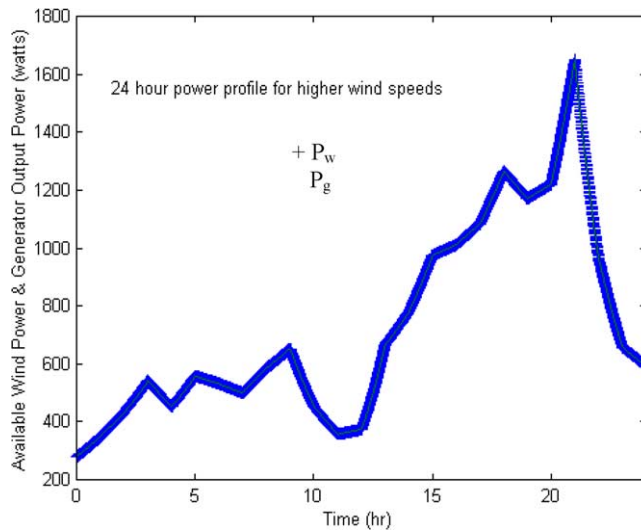


Fig. 4. Maximum power tracking for higher wind speed profile.

output power, which proves that the controller forces the system to extract the maximum power and deliver it as useful electric energy. Fig. 5 shows the output dc voltage of BB2 when a step change of 7 V in the reference voltage is applied. It is clear that the output voltage follows the reference value, i.e. accurate tracking of the output voltage is achieved via FLC2. The corresponding values of  $d_1$  and  $d_2$  for maximum power tracking and output voltage regulation in winter are shown in Figs. 6 and 7, respectively.

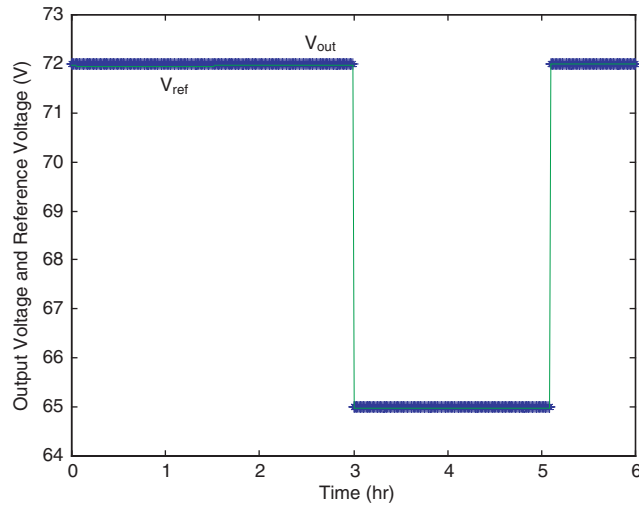


Fig. 5. FLC2 tracking at step change in reference voltage.

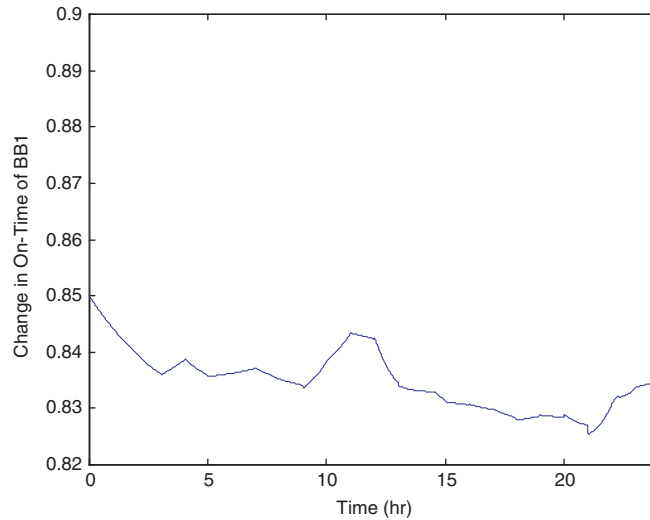


Fig. 6. On time of first buck boost converter for high wind speeds.

## 2.6. PV subsystem

Fig. 8 shows the block diagram of the PV subsystem proposed in this paper. The PV array used consists of 40 modules, each of which deliver 56 W peak power (17.7 V and 3.16 A at STC). To satisfy the required load of 72 bus voltage, four of the modules are connected in series and ten in parallel to obtain the 2.24 kW peak power.

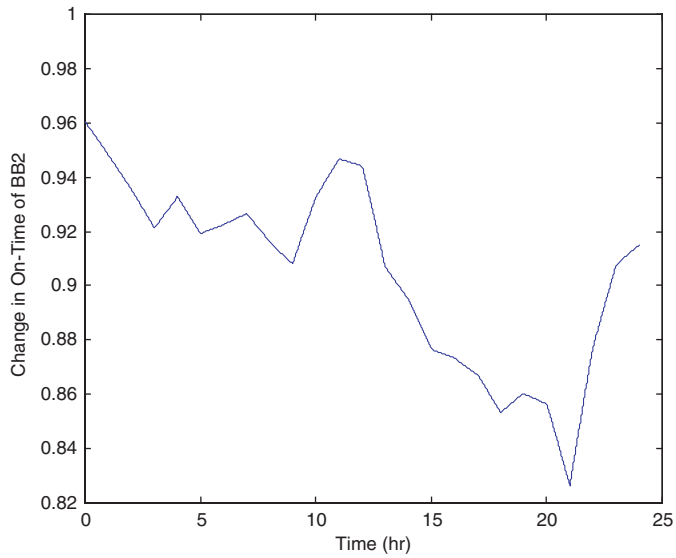


Fig. 7. On time of second buck boost converter for high wind speeds.

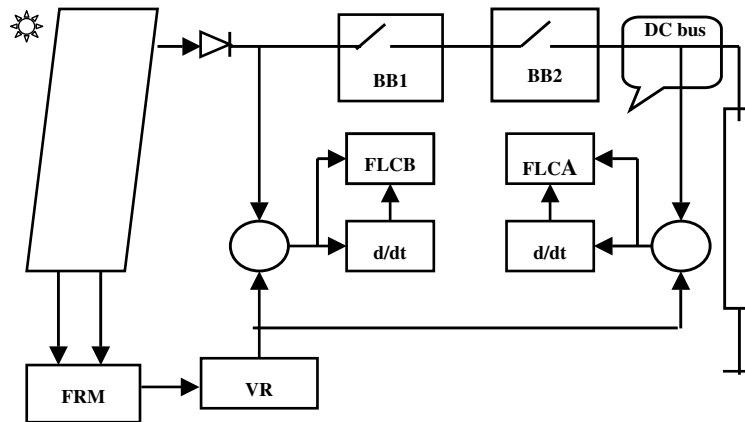


Fig. 8. Block diagram of the PV subsystem.

### 2.7. MPP determination

To maximize the power extracted from the PV system, the MPP voltage  $V_m$  and current  $I_m$  are determined on line using a fuzzy regression model (FRM) [9–19]. The FRM is based on the linear possibility system using symmetrical fuzzy numbers  $A_i = (\alpha_i, c_i)$ , where  $\alpha_i$  is the center and  $c_i$  is the width of the reference function  $L(x)$ , which is expressed as

$$Y = A_0 + A_1X_1 + A_2X_2 + \dots + A_nX_n \tag{10}$$

where  $A_0$  is a fuzzy constant,  $X$  is the input variables system and  $Y$  is the system output. For both models of  $V_m$  and  $I_m$  determination, the fuzzy model input parameters are; the solar insolation incident on the array surface “ $W$ ” and the panel surface temperature “ $T$ ”.

### 2.8. Buck boost converters

The same type of converters illustrated in Section 2.4 is also used in the PV subsystem for power control. Two dc–dc buck boost converters are used. The first one is used to achieve the MPP (their parameters are denoted with  $A$ ). The second is used to supply the 72 V dc load voltage (their parameters are denoted with  $B$ ).

### 2.9. FLC for PV subsystem

Because of the non-linearity of the PV solar cells, non-deterministic solar cell parameters and shortage of available manufacturer data about the system, application of FLC is necessary. Two FLCs are designed to achieve the following goals for the PV subsystem:

1. Fuzzy logic controller (FLCA) varying the on time ( $d_A$ ) of the switching device of the first buck boost converter (BBA) for MPP tracking. The inputs to FLCA are chosen to be the error between the PV generator power and the determined MPP through the application of the FRM, defined as “error”, and the change in this error “cerror”. FLCA output is the new value of  $d_A$ .
2. Fuzzy logic controller (FLCB) varying the on time ( $d_B$ ) of the switching device of the second buck boost converter (BBB) for regulating the output voltage of the PV subsystem. The inputs to FLCB are chosen to be the error between the reference voltage and the actual output voltage from the first converter (error) and the change in this error (cerror). FLCB output is the new value of  $d_B$ .

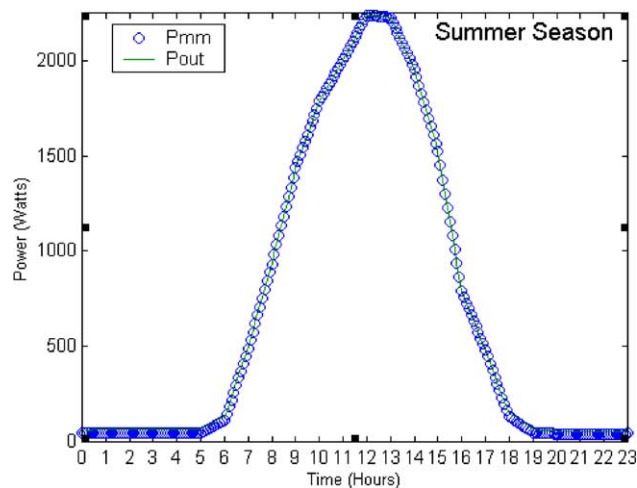


Fig. 9. MPP and output power from BBA at summer.

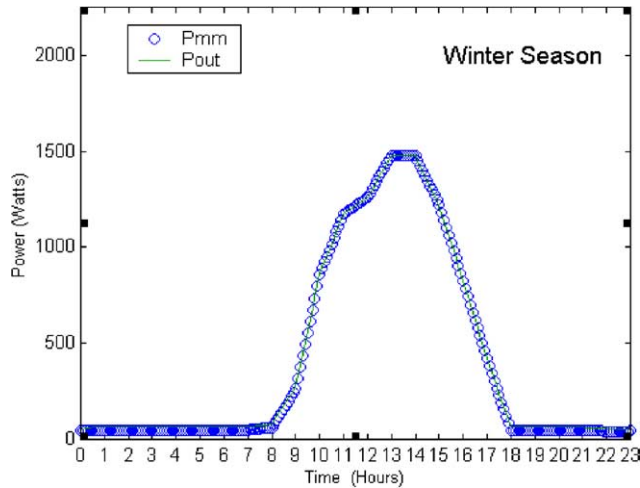


Fig. 10. MPP and output power From BBA at winter.

Seven uniformly distributed triangular membership functions are used for the “error” and “error” inputs and the outputs from both FLCs.

Figs. 9 and 10 show the measured solar insolation measurements at the El-Hammam site during two seasons (summer and winter, respectively) of 1996. These two extremes are used to test our FLC system and the desired requirements of the MPP tracking for the first converter BBA and the dc bus voltage for the second one (BBB). Figs. 9 and 10 show the good traceability of the MPP with varying insolation during the day and also with changes in the insolation levels. Fig. 11 shows the on time of BBA for low insolation level (winter season). Fig. 12 shows the 10 V step down change in the reference signal during a period from 8:00 to 11:00 (3 h), the output

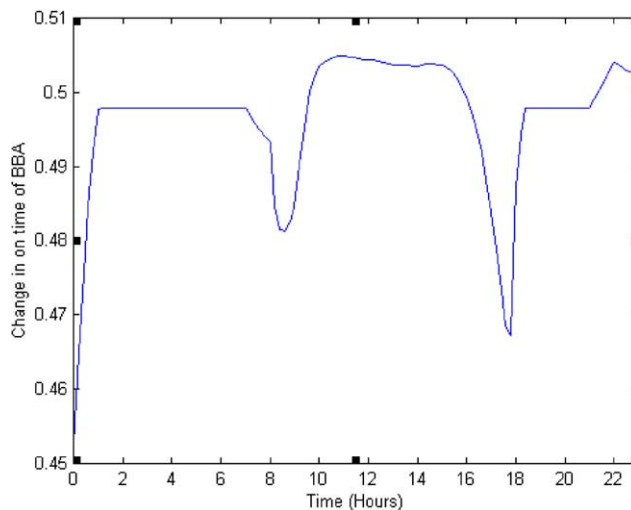


Fig. 11. On time of BBA for low insolation level.

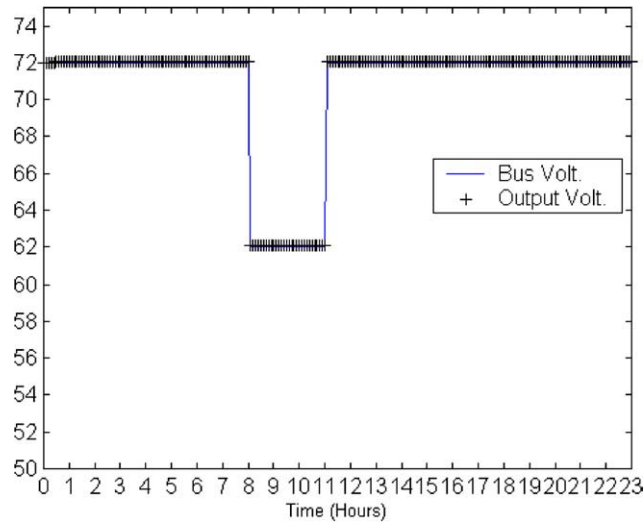


Fig. 12. FLCB tracking at step change in reference voltage.

voltage from the BBB and the corresponding  $d_B$ . As shown, an accurate output voltage tracking is achieved via FLCB.

### 2.10. Electrolyzer subsystem

The Unipolar Stuart cell is a high efficiency, low maintenance, rugged and reliable cell. Each electrode has a single polarity, producing either  $H_2$  (cathode) or  $O_2$  (anode). The electrolyzer consists of a number of cells isolated from one another in separate cell compartments. Cell voltage under normal operating conditions is in the range of  $1.7\text{--}1.9V_{dc}$  [7]. Generated hydrogen is stored in a tank. The inlet and outlet of the tank are controlled via the management system, which monitors the hydrogen pressure as well.

### 2.11. Fuel cell subsystem

A proton exchange membrane (PEM) fuel cells stack is used. The PEM uses a polymer membrane as its electrolyte [7]. In the proposed system, air is used as the oxidant; the cell pressure is atmospheric and the cell temperature is  $70^\circ\text{C}$ . The current density is designed as  $400\text{ mA/cm}^2$ . This leads to using 576 fuel cells in the stack.

## 3. System management

### 3.1. Management algorithm

The data from the Al-Hammam site on the North Coast is used in the case study. The data includes wind speeds, wind direction, solar insolation and temperature throughout the whole year. The total wind and solar energy generated simultaneously is calculated and plotted in Fig. 13 for

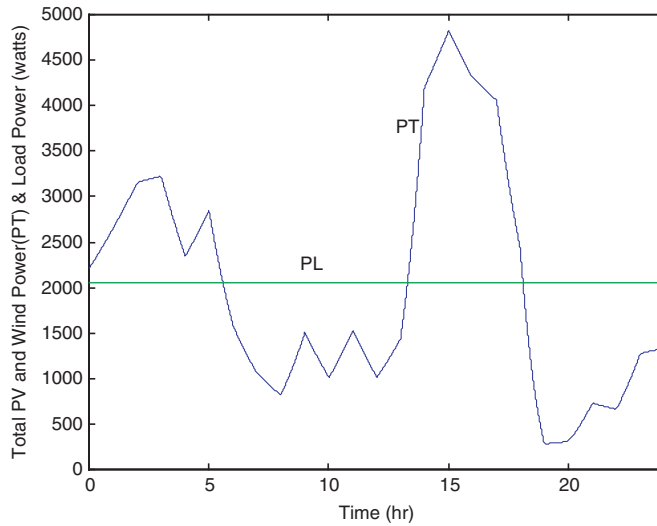


Fig. 13. Renewable sources power PT and load power PL.

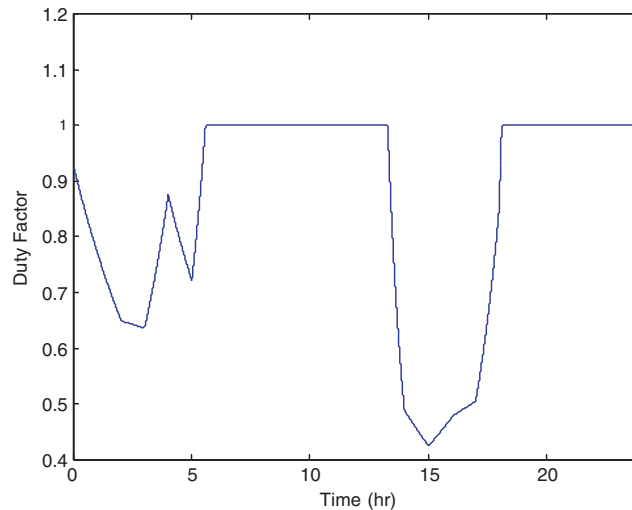


Fig. 14. Duty factor.

the winter season. On the same plot, the load power demand is drawn. Fig. 14 plots the duty factor “ $D$ ” following the available wind and solar generation. “ $D$ ” takes the value ONE when the load demand is higher than the total generation and takes values less than ONE when the load demand is less than the total generation. This is clear when relating Figs. 13 and 14 to each other.

Knowing the load demand, the surplus energy is determined. The surplus energy is used to generate hydrogen from the electrolyzer, which is stored in tanks. At the times when both the wind and PV sources are unable to supply the load demand, the stored hydrogen is supplied to the fuel cells (FC). The managing system controls the operation of the FC modules to supply the

deficiency in the load demand. Load shedding is allowed if the total power generated is less than the load demand.

The fuel cell module is shown in Fig. 15. The fuel cell module comprises four FC units, namely A1, A2, A3 and A4. The module is designed such that A1 can supply 50% of the load demand, A2 can supply 25% of the load demand and each of A3 and A4 can supply 12.5% of the load demand. Hence, the FC module can supply the full load in case of complete shortage of the renewable energy supply.  $V_{1H}$  to  $V_{4H}$  shown on this figure are the valves controlling the hydrogen flow to the fuel cell and are controlled by the fuel cell control bus.  $V_{1O}$  to  $V_{4O}$  shown on the figure are the valves controlling the oxygen flow to the fuel cells and are controlled by the fuel cell control bus.  $S_1$  to  $S_4$  are switches connecting the fuel cell current to the dc bus and are also controlled

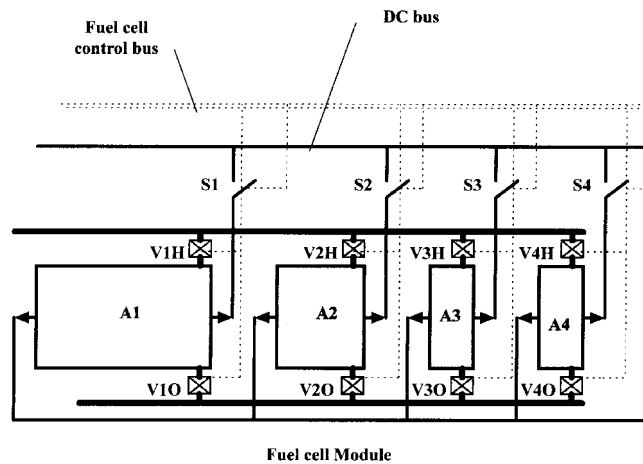


Fig. 15. Fuel cells module.

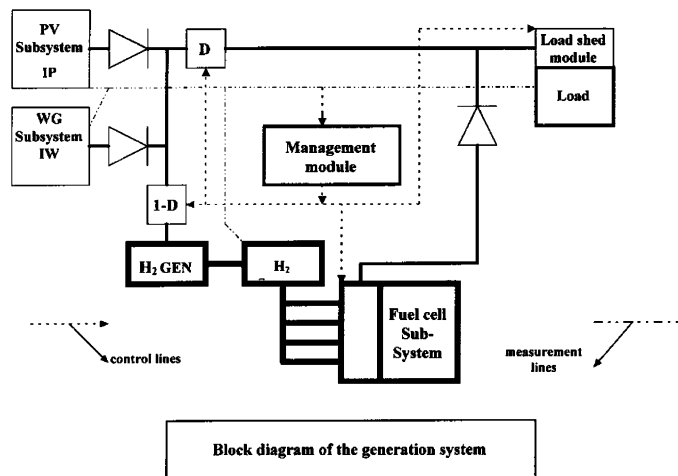


Fig. 16. Generation system layout.

by fuel cell control bus. Fig. 16 demonstrates the role of the management module in controlling the flow of power from the PV, wind and FC subsystems to the load. The management module monitors the PV power, wind power, load power and hydrogen tank pressure and issues commands determining the duty factor as well as the states of the different valves and switches of the FC module shown in Fig. 15. The flow chart describing the management of the power flow in the proposed system is shown in Fig. 17.

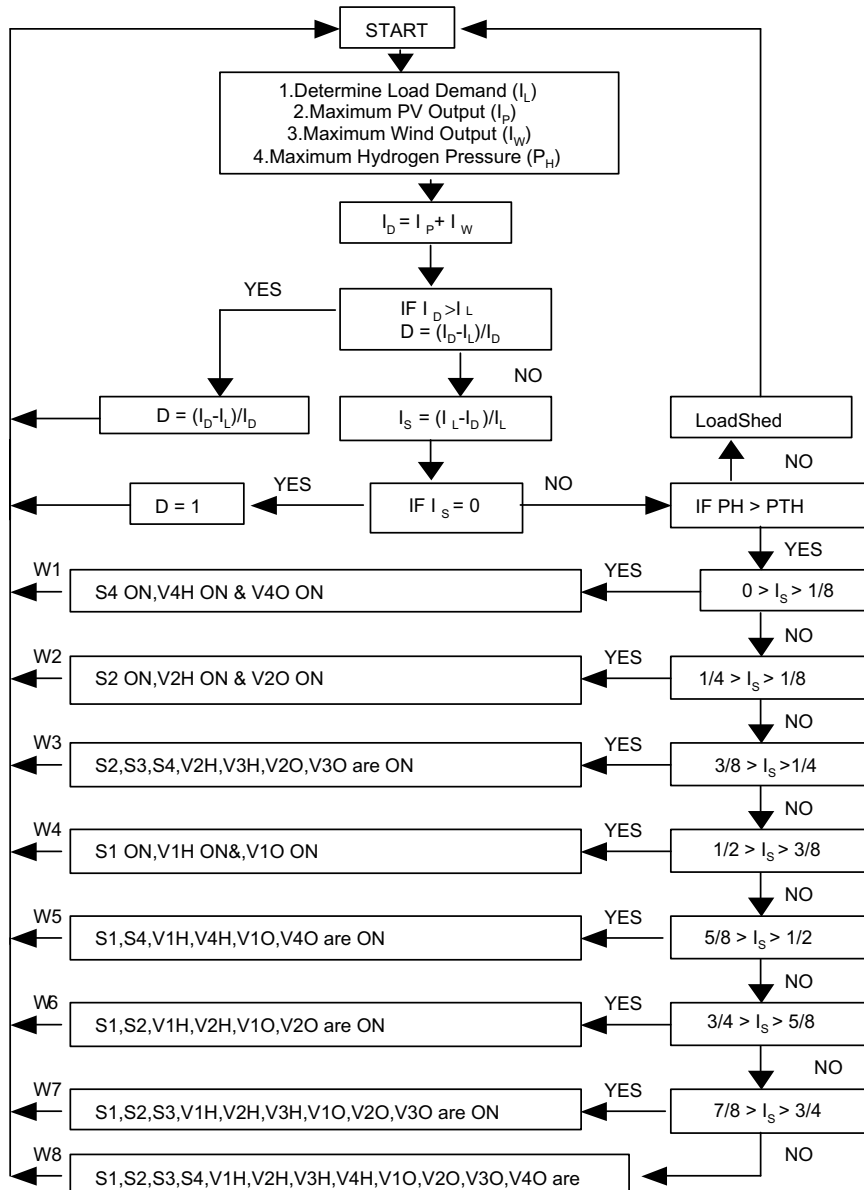


Fig. 17. Flow chart of system management.

### 3.2. Simulation results

Simulation results showing the states of the different switches are shown in Fig. 18 for the case of data taken in 1996 on the El-Hammam site. The results are shown as:  $W_i = [V_{iH}, V_{iO}, S_i]$  where  $i = 1, 2, \dots, 8$  are the states of the management system described in the flow chart. Valves and switches control is achieved via comparator circuits, which is activated simultaneously.

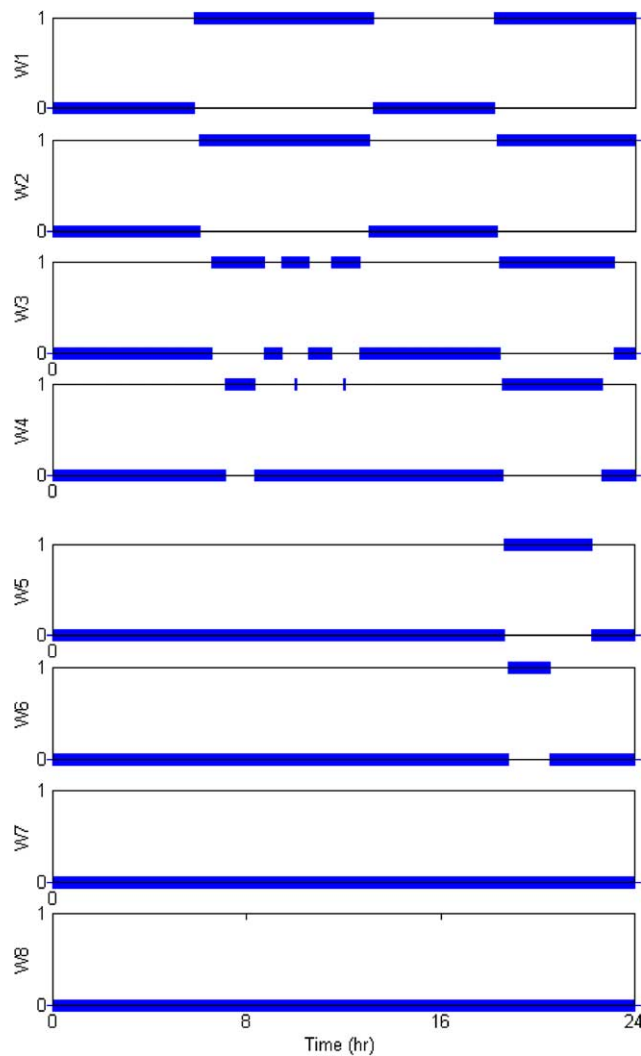


Fig. 18. Status of valves and switches for 24 h in January.

#### 4. Conclusion

In this paper, an energy system comprising three energy sources, namely PV, wind and fuel cells, is proposed. Each of the three energy sources is controlled so as to deliver energy at optimum efficiency. Fuzzy logic control is employed to achieve maximum power tracking for both PV and wind energies and to deliver this maximum power to a fixed dc voltage bus. The results obtained from the research work are as follows:

1. The feasibility of using fuzzy logic controllers for tracking the maximum power available in both wind and PV energy systems is demonstrated.
2. The accuracy of the fuzzy logic controllers in regulating the dc bus voltage in the whole range of wind speeds and solar insolation obtained from the considered site data is proved. This is done by studying the change in output voltage following an abrupt change in wind speed and/or solar insolation in the presence of the controllers.
3. The proposed system for managing the flow of power is simulated using the El-Hammam on site data. The data includes wind speed and PV insolation.

#### References

- [1] Simoes MG, Bose BK, Spiegel R. Fuzzy logic based intelligent control of a variable speed cage machine wind generation system. *IEEE Trans. PE* 1997;12(1):87–94.
- [2] Fernao V, Amaral T, Fernando J, Crisostomo M. Fuzzy logic control of a single phase ac/dc buck-boost converter. In: *Proceedings of EPE conference, Switzerland, 1999*, p. 1–10.
- [3] El-Shatter TF. Tracking inverter design for a solar cell system, MSc Thesis, Cairo University, 1991.
- [4] Elhagry MT, Saleh MB, Abouelzahab EM, Elkousy AA, El-Shatter TF. Modelling of PV system equivalent circuit using fuzzy regression. *Midwest conf, Aug, USA, 1997*.
- [5] El-Shater TF. Fuzzy modeling and simulation of photovoltaic systems. PhD Thesis, Cairo Univ, Faculty of Eng, 1998.
- [6] El-Shater TF, Eskander M, El-Hagry M. Hybrid pv/fuel cell system design and simulation. In: *36th intersociety energy conversion engineering conference, Savannah, Georgia, July 29–August 2, 2001*.
- [7] Leuven KU. *Wind energy for the eighties*. Stevenage, UK: Peter Peregrinus Ltd; 1982.
- [8] Ryan MJ, Lorenz RD. A novel control-oriented model of a PM generator with diode bridge output. In: *Proceedings of EPE conference, Trondheim, Norway, 1997*, p. 324–9.
- [9] Lee Y-S. *Computer aided analysis and design of switch mode power supplies*. NY: Marcel Dekker Inc; 1993.
- [10] Green MA. *Solar cells: operating principles, technology, and system applications*. Englewood Cliffs, NJ: Prentice-Hall, Inc; 1982.
- [11] Zadeh LA. *Fuzzy sets, information and control*, vol. 8, p. 335–53.
- [12] Yu G, Song J, Kim S. Development of power converter for photovoltaic system. *Japan–Korea Joint Seminar, Toejon, Korea, May 22–23, 1995*.
- [13] Pell W, Donepudi VS, Adams WA. An experimental study of a PV system including a zinc/bromine battery. In: *11th E.C.PV solar energy conference, Switzerland, 12–16 October, 1992*.
- [14] Groumpos PP. PV power systems: a brief introduction. In: *Proceedings of the American control conference, 1983*.
- [15] Fox Da, Shuey KC, Stechschulte DL. Peak power tracking technique for PV arrays. *IEEE power electronics specialists conference, 1979*.
- [16] Gordon JM, Wenger HJ. On optimizing central-station PV solar power systems: the role of field layout, shading, tracking, and array geometry. *Solar World congress, Denver, CO, 1991, USA*.

- [17] Runyan WR. Semiconductor measurements and instrumentation. Texas Instruments Incorporated, 1975.
- [18] Hanel A, Imamura MS. Improvement of PV array performance. In: 11th E.C. PVSEC, Switzerland, 12–16 October, 1992.
- [19] Terano T, Asai K, Sugeno M. Fuzzy systems theory and its applications. USA: Academic Press, Inc; 1992.